*DOI:*
10.1016/j.ajpath.2017.08.022

*Document Version*
Peer reviewed version

**Myofilament remodeling and function is more impaired in peripartum cardiomyopathy compared to dilated cardiomyopathy and ischemic heart disease**

Ilse Anne Elise Bollen[1,2], Elisabeth Ehler[3], Karin Fleischanderl[3], Floor Bouwman[1], Lanette Kempers[1], Melanie Ricke-Hoch[4], Denise Hilfiker-Kleiner[4], Cristobal Guillermo dos Remedios[5], Martina Krüger[6], Aryan Vink[7], Folkert Wouter Asselbergs[8,9,10], Karin Yvon van Spaendonck-Zwarts[2,11], Yigal Martin Pinto[2,12], Diederik Wouter Dimitri Kuster[1, 2,], Jolanda van der Velden[1, 2,13]

[1]Department of Physiology, VU University Medical Center, Amsterdam, the Netherlands.

[2]Amsterdam Cardiovascular Sciences, Amsterdam, the Netherlands

[3]Randall Division of Cell and Molecular Biophysics and Cardiovascular Division, British Heart Foundation Centre of Research Excellence, King's College London, United Kingdom.

[4]Department of Cardiology and Angiology, Hannover Medical School, Hannover, Germany.

[5]Bosch Institute, Discipline of Anatomy & Histology, University of Sydney, Sydney, Australia.

[6]Institute of Cardiovascular Physiology, Heinrich-Heine University Düsseldorf, Düsseldorf, Germany.

[7]Department of Pathology, University Medical Center Utrecht, Utrecht, the Netherlands.

[8]Department of Cardiology, Division Heart & Lungs, University of Utrecht, University Medical Center Utrecht, Utrecht, the Netherlands.

[9]Durrer Center for Cardiogenetic Research, ICIN-Netherlands Heart Institute, Utrecht, the Netherlands.

[10]Institute of Cardiovascular Science, Faculty of Population Health Sciences, University College London, London, United Kingdom.

[11]Department of Clinical Genetics, Academic Medical Center Amsterdam, University of Amsterdam, Amsterdam, the Netherlands.

[12]AMC Heart Center, Department of Clinical and Experimental Cardiology, Academic Medical Center Amsterdam, University of Amsterdam, Amsterdam, the Netherlands.

[13]Netherlands Heart Institute, Utrecht, the Netherlands.

**Corresponding author:**

Ilse Bollen

Dept. of Physiology
VU University Medical Center
De Boelelaan 1117, room 11W53
1081 HV Amsterdam, the Netherlands
Phone: +31627339910
e-mail: a.bollen@vumc.nl

Running head: PPCM differs from DCM and ISHD

Number of text pages: 28

Number of figures: 6

Funding: Dutch Heart Foundation CVON2011-11 ARENA, British Heart Foundation, Rembrandt Institute for Cardiovascular Sciences 2013, Dekker Scholarship-Junior Staff Member 2014T001 – Netherlands Heart Foundation and UCL Hospitals NIHR Biomedical Research Centre.

Disclosures: None declared.

**Abstract**

Peripartum cardiomyopathy (PPCM) and dilated cardiomyopathy (DCM) show similarities in clinical presentation. However, while DCM patients do not recover and slowly deteriorate further, PPCM patients show either a fast cardiac deterioration or complete recovery. The aim of this study was to assess if underlying cellular changes can explain the clinical similarities and differences in the two diseases. We therefore assessed sarcomeric protein expression, modification, titin isoform shift, and contractile behavior of cardiomyocytes in heart tissue of PPCM and DCM patients and compared these to non-failing controls. Heart samples from ischemic heart disease (ISHD) patients served as heart failure control samples. Passive force was only increased in PPCM samples compared to controls while PPCM, DCM and ISHD samples all showed increased myofilament $Ca^{2+}$-sensitivity. Length-dependent activation was significantly impaired in PPCM compared to controls, while no impairment was observed in ISHD samples and DCM showed an intermediate response. Contractile impairments were caused by impaired PKA-mediated phosphorylation since exogenous PKA restored all parameters to control levels. While DCM samples showed re-expression of EH-myomesin, an isoform usually only expressed in the heart before birth, PPCM and ISHD did not. The lack of EH-myomesin, combined with low PKA-mediated phosphorylation of myofilament proteins and increased compliant titin isoform, may explain the increase in passive force and blunted length- dependent activation of myofilaments in PPCM samples.

## Introduction

*Clinical presentation*

Dilated cardiomyopathy (DCM) and peripartum cardiomyopathy (PPCM) are distinct forms of cardiac disease that share aspects of clinical presentation such as dilated ventricle(s), reduced systolic function and cardiac rhythm disorders[1, 2]. PPCM is a cardiac disease that presents itself during the last month of pregnancy, during delivery or within the first 5 months post partum[2]. A genetic cause for both DCM and PPCM has been demonstrated before[3-6]. Evidence has accumulated showing that about 15-20% of PPCM patients carry cardiomyopathy-causing mutations mainly in *TTN*, *MYH7* and *SCN5A*, genes in which mutations are associated with DCM as well[3]. PPCM patients are often young and show fast cardiac deterioration after disease onset leading to the need for heart transplantation or death[7-10]. In contrast, DCM patients develop cardiac disease at older age with a milder disease progression compared to PPCM[11]. While PPCM patients can show fast cardiac deterioration, they often can be stabilized or even show complete recovery upon treatment[7-14]. In a cohort of 182 PPCM patients in the United States of America 27% showed full recovery, while 25% experienced at least one major adverse event, defined as death or complications that were life-threatening or lead to long-term morbidity[15]. Of the patients who survived a major adverse event, but did not receive a cardiac transplantation, 7 (32%) suffered from residual brain damage. Of the cohort 13 patients died within 8 years, of which 5 suddenly, and 11 underwent cardiac transplantation within 2 years after diagnosis. Cardiopulmonary arrest occurred in 6 patients either during delivery or within the first 6 days after delivery. Severe pulmonary edema requiring intensive care occurred in 16 patients within one week after delivery[15]. This cohort clearly illustrates the fast cardiac deterioration in PPCM patients. A German cohort of 115 PPCM patients reported an improvement rate of 85%, full recovery rate of 47%, a 15% failure to recover and death in 2%[13], demonstrating the high recovery rate from PPCM[13]. DCM patients may be stabilized, but recovery after treatment is unlikely[6, 14].

*Pathogenesis*

Interestingly, DCM patients who become pregnant are more likely to experience adverse cardiac events such as heart failure, sustained arrhythmia, or stroke earlier in pregnancy[16] than PPCM patients. This is likely caused by an increased hemodynamic load on an already troubled heart. In contrast, increased cardiac strain does not

appear to be a disease trigger for PPCM as the highest incidence of disease onset is not at the time of the largest increase in hemodynamic load (approximately 24 weeks), but rather in the first month postpartum[10]. In addition, it has been shown that the hormone prolactin plays a key role in PPCM pathogenesis. High levels of oxidative stress induces cleavage of the breast-feeding hormone prolactin into a 16 kDa fragment that has detrimental effects on cardiac function[7, 17, 18]. The peak of prolactin levels coincides with the peak incidence of disease onset in PPCM and while prolactin levels are low in non-pregnant and non-nursing individuals[19], it is unlikely that prolactin plays a role in DCM. A recent study suggests detrimental effects of catecholamine treatment, specifically with the β1-adrenergic receptor agonist dobutamine in PPCM patients[13, 20]. In fact, experimental data showed that β1-receptor agonist isoproterenol impaired fatty acid and glucose uptake[20]. The resulting energy depletion increased production of reactive oxygen species and led to cardiomyocyte death and progression of heart failure in STAT3 knock out mice which could be attenuated with β-blocker metoprolol[20]. Based on differences in disease onset and progression, we hypothesize that different cellular remodeling underlies PPCM and DCM.

We studied myofilament functional and structural remodeling in PPCM and DCM compared to ischemic heart disease (ISHD) and non-failing controls to define common and unique pathomechanisms for PPCM and DCM. We show that both PPCM and DCM patients suffer from increased myofilament $Ca^{2+}$-sensitivity and reduced myofilament length-dependent activation compared to controls. The changes in PPCM samples were more severe than observed in DCM samples, while ISHD samples only showed an increased $Ca^{2+}$-sensitivity without an impairment in length-dependent activation. In addition, PPCM patients showed a significant increase in passive force ($F_{pass}$) development compared to controls, while DCM and ISHD samples showed similar $F_{pass}$ as controls. Also myofilament remodeling was different between DCM and PPCM patients. While both patient groups showed a similar increase in compliant titin and fibrosis, only DCM patients expressed the EH-myomesin isoform which could have contributed to the observed differences in contractile force of myofilaments. The lack of a stabilizing effect of EH-myomesin in PPCM may play a key role in the short-term fast disease progression observed in PPCM. On the other hand, limited remodeling might also explain total recovery in a large group of PPCM patients.

**Methods**

*Ethical approval*

Left ventricular (LV) tissue from DCM, PPCM and ISHD samples were acquired from the University of Sydney, Australia, with the ethical approval of the Human Research Ethics Committee #2012/2814. The codes of used samples are; DCM: 3.107, 4.036, 3.133, 4.125, 2.082 and 3.042, PPCM samples: 2.048, 3.058, 3.118, 4.127, ISHD samples: 4.111, 4.108, 4.070, 4.091. As control samples we used explanted LV heart tissue of healthy donors; people died from a non-cardiac cause, typically motor vehicle accidents. These healthy donor samples were also acquired from the University of Sydney, Australia and samples included are: 3.162, 6.042, 3.141, 3.164, 5.086, 6.034, 8.004, 7.040, 7.054, 6.008, 5.128, 7.044, 4.104, 6.020, 3.160 and 6.056. In addition, 2 DCM samples were acquired from the Biobank of the University Medical Center Utrecht, the Netherlands. This study was approved by the Biobank Research Ethics Committee, University Medical Center Utrecht, Utrecht, the Netherlands (protocol number WARB 12/387). Written informed consent was obtained. Of the PPCM samples, 2 samples were acquired from at the University of Hannover, Germany. One sample was obtained during implantation of LV assist device during the acute phase of PPCM and the other after cardiac transplantation after chronic heart failure. PPCM tissue analyses were approved by the local ethics commission of the Hannover Medical School, both patients provided written informed consent. All samples were stored in liquid nitrogen or at -80$^{o}$C until use.

*Fibrosis*

Cryosections of 5 µm were stained with picro-Sirius red. The amount of fibrosis was quantified using ImageJ version 1.49. The fibrotic area was selected using Huang thresholding method, threshold colour red, colour space RGB, wide open blue and red filters and adjusted green filter to distinguish stained from non-stained areas. The percentage of fibrosis was calculated as the percentage of red stained tissue relative to the total area of the picture analysed. Of each sample at least 3 pictures were taken and data are shown as the average per sample.

*Cardiomyocyte force measurements*

Maximal force ($F_{max}$) and passive force ($F_{pass}$) of sarcomeres were measured at pCa 4.5 and pCa 9.0 respectively in single membrane-permeabilized cardiomyocytes mechanically isolated from heart tissue as previously described[21, 22]. Briefly, a small piece of tissue (10-15 mg) was defrosted in 4$^{o}$C isolation relax solution containing

1 mM free Mg, 139.6 mM KCl, 2 mM EGTA, 5.95 mM ATP and 10 mM imidazole with pH adjusted to 7.0 with KOH. The tissue was cut in small pieces and mechanically disrupted with a Teflon piston for 5-10 seconds at 900 rpm to obtain a suspension of single cells, small clumps of cells and cell fragments. In order to permeabilize the membranes the cell were incubated with 0.5% TritonX-100 (Millipore) for 5 minutes at 4°C. Cells were washed with isolation relax solution to remove Triton and kept at 4°C until measurement on the same day. Single cardiomyocytes were selected for measurement based on size (100-150 µm long and 10-35 µm in diameter) and uniformity of striation pattern. Single cardiomyocytes were attached to stainless steel needles attached to a force transducer and a length motor with silicon based glue (DB-025, Zwaluw, Den Braven) while being viewed with an inverted microscope at 320x magnification. Sarcomere length was determined by spatial Fourier transformation and set at the desired sarcomere length prior to force measurement starting with the smallest sarcomere length. The relax (pCa 9.0) and activation (pCa 4.5) solutions contained respectively 6.48 and 6.28 mM MgCl, 5.89 and 5.97 mM $Na_2ATP$, 6.97 and 0 mM Ethylene glycol-bis(2-aminoethylether)-N,N,N′,N′-tetraacetic acid (EGTA) and 0 and 7 mM $Ca^{2+}$–EGTA. Both relax and activation solution also contained 14.5 mM creatine phosphate and 100 mM N,N-bis[2-hydroxyethyl]-2-aminoethane-sulphonic acid of which the pH was adjusted to 7.1 with KOH. The ionic strength of the solutions were adjusted to 200 mM with potassium propionic acid. The submaximal pCa solutions were created by appropriate mixing of the relax and activation solutions. A single batch of pCa solutions was used for all active force measurements in this study in order to eliminate bias due to batch-to-batch variation. All passive and active force measurements were performed at 15°C to assure stability of the cell during measurement and temperature was controlled with a circulating water bath. For active force measurements cells were transferred to the desired pCa ($-\log[Ca^{2+}]$) and force development was recorded until steady state had been reached. Cells were then shortened with 30% of cell length in order to detach cross bridges and to determine total force development. Cells were then transferred back to a relax solution and shortened again with 30% of cell length in order to calculate passive force development. Active force development was calculated by substraction of passive force from total force. Force was measured in activation solution (pCa 4.5) first to obtain maximal force development and thereafter at different pCa solutions in a random order. Finally, force was measured again in activation solution in order to confirm the cardiomyocyte did not suffer from inappropriate reduction in maximal force during measurement protocol. Relative forces during experiment were corrected for decrease in maximal force during the protocol and measurements were excluded if the decrease in force was >30%. Passive force curves were measured by

stretching the cell to various sarcomere lengths and measurement of passive force in relax solution. All forces were normalized to cross sectional area of the cardiomyocytes, calculated as (width* depth*π)/4, at a sarcomere length of 2.3µm. Protein kinase A (PKA) incubations were performed as previously described[22]. In short, membrane permeabilized cardiomyocytes were incubated with 80 µl 1unit/µl PKA (P5511, Sigma) with 0.006 mM cAMP (Sigma) in isolation relax solution at 20°C for 40 minutes prior to measurement of force at 15°C according to the same protocol described above without prior PKA incubation. Relative force-[$Ca^{2+}$] curves were constructed and $Ca^{2+}$-sensitivity was measured as the [$Ca^{2+}$] needed to achieve 50% of $F_{max}$ ($EC_{50}$) and length-dependent activation was measured as the shift in $EC_{50}$ ($\Delta EC_{50}$) at a sarcomere length of 1.9 µm and 2.3 µm. A representation of how $EC_{50}$ and $\Delta EC_{50}$ were calculated can be found in Supplemental Figure S1. The number of cardiomyocytes measured in each experiment is indicated as "n" and the number of patients these cardiomyocytes were derived from are indicated as "N" in figure legends.

*Protein expression and modification*

Titin isoforms were separated on a 1% (w/v) agarose gel and stained with SYPRO Ruby protein gel stain (Invitrogen) as described previously[23] and samples were measured in triplicate.

The size of N2BA titin was calculated as described previously[24, 25]. In short, homogenates of the samples of interest (PPCM, DCM and ISHD) were loaded adjacent to a non-failing control heart and soleus muscle of an adult mouse on a 1% agarose gel and proteins were separated in the same way as described above for titin isoform composition. A calibration curve was constructed based on mobility of proteins of known molecular weight (N2A soleus 3690 kDa; N2B non-failing heart 2970 kDa; nebulin soleus muscle 748 kDa and myosin heavy chain (MHC) 200 kDa) relative to MHC. This calibration curve was used to calculate the molecular weight of the N2BA titin band of the sample of interest based on relative mobility to MHC. An example of a calibration curve and the associated calculation to determine titin N2BA size is depicted in Supplemental Figure S2A, B. In order to avoid gel-to-gel variation or variation in mobility within a gel, only the adjacent lanes were used for the construction of the calibration curve. For all samples the same reference control sample was used and all samples were measured in duplicate.

To assess titin phosphorylation homogenates were loaded on a 2.1% acrylamide, 0.5% agarose-strengthened gel and separated as previously described[26]. Proteins were transferred to a PVDF membrane, blocked with 3% BSA and incubated with phospho site-specific antibodies directed to Serine-4010 (Ser4010; N2Bunique

sequence (N2Bus) domain; PKA and extracellular signal-regulated kinase 2 (ERK2) target), or Serine-12022 (Ser12022; PEVK domain; protein kinase C (PKC) and $Ca^{2+}$/calmodulin dependent protein kinase II (CaMKIId) target) both from Eurogentech, Belgium. Incubation of primary antibodies was followed by incubation with secondary HRP-conjugated antibody. Enhanced chemiluminescence detection kit (Amersham) was used in order to detect phosphorylated proteins with the Fuji-imager LAS 4000 imager. Membranes were stripped to remove phospho-specific antibody and blocked again with 3% BSA. Membranes were then incubated with an antibody directed to total titin (Eurogentech, Belgium) and visualized with enhanced chemiluminescence detection kit (Amersham).

Phosphorylation of cardiac troponin I (cTnI) and cardiac myosin binding protein C (cMyBP-C) were assessed as previously described[27]. Phosphorylation of cTnI was further studied by phos-tag analysis in which non-, mono- and bis-phosphorylated cTnI (Pierce, MA1-22700) were separated by polyacrylamide bound $Mn^{2+}$-phos-tag gel electrophoresis western blotting as previously described[28].

Glutathionylation of cMyBP-C was assessed as previously described[29] with minor deviations from protocol. In short: A non-reducing RIPA buffer was used for protein isolation to which 25 mM N-ethylmaleimide (NEM) (Sigma) was added prior to isolation. After protein isolation, the homogenate was diluted in a 1:1 ratio with 2x Laemmli sample buffer and loaded on Criterion™ TGX™ Precast gels 8-16% (BioRad). Proteins were transferred to nitrocellulose membrane (BioRad) and blocked with 5% blocking grade buffer containing 2.5 mM NEM. Membranes were cut and incubated with antibodies against glutathione (Sigma, ab19534) or GAPDH (14C10 Cell signaling). Membranes were stripped (Restore™ Western Blot Stripping Buffer, Thermo Scientific), blocked with 5% blocking grade buffer and incubated with antibody against cMyBP-C (sc-67354, Santa Cruz) followed by incubation with secondary HRP-conjugated antibody. Enhanced chemiluminescence kit (Amersham) was used to detect proteins with the Amersham imager 600. As positive and negative controls for the glutathione western blot, cardiomyocytes were isolated from a male Wistar rat (200g). The animal experiments were performed in accordance with the guidelines from Directive 2010/63/EU of the European Parliament on the protection of animals used for scientific purposes. Liberase TM[30] was used for isolation of adult rat cardiomyocytes and cells were suspended in plating-medium containing medium 199 (Lonza), penicillin/streptomycin (1%) and fetal bovine serum (5%). Cardiomyocytes were carefully pipetted on laminin coated glass coverslips. One hour after plating, cells that were not attached were removed by replacing the plating-medium with culture-medium that consisted of medium 199, penicillin/streptomycin (1%) and ITS

supplement (Sigma Aldrich,insulin 10 mg/l, transferrin 5.5 mg/l, and selenium 5 µg/l). Positive controls were rat cardiomyocytes incubated for 1 hour with various concentrations of the membrane-permeable thiol oxidizing agent diamide (Sigma). Negative controls were homogenates from rat cardiomyocytes treated with the reducing agents 100 mM dithiothreitol (DTT) and 1.4 M β-mercaptoethanol (BME) prior to loading. The glutathione western blot was confirmed to work since adding DTT and BME reduced the glutathione signal and adding diamide in non-reducing conditions increased the glutathione signal in a dose dependent manner (Supplemental Figure S3A, B).

*EH-myomesin expression immunohistochemistry*

Human heart tissue pieces were cut on a Leica CM 1950 cryostat and 12 µm thick sections were retrieved on poly-lysine coated slides and dried overnight. Sections were fixed for 5 min in acetone at -20°C, followed by brief rehydration in PBS and 30 min blocking in 5% preimmune goat serum (Sigma)/1% bovine serum albumin (BSA, Sigma) in gold buffer (GB; 20 mM Tris-HCl, pH 7.5, 155 mM NaCl, 2 mM ethylene glycol tetraacetic acid [EGTA], 2 mM $MgCl_2$). Mouse monoclonal anti myomesin (clone B4[31]) and rabbit polyclonal anti human EH-myomesin (Schoenauer et al., 2011; PMID 21069531; generously donated by Dr Irina Agarkova) were diluted in 1% BSA/GB and incubated overnight in a humid chamber. After 3x 5 min wash in PBS, secondary antibodies (Cy3-goat anti mouse immunoglobulins and Cy2-goat anti rabbit immunoglobulins; both multilabelling quality from Jackson Immunochemicals via Stratech Scientific, UK) and DAPI were incubated for 30 min at room temperature in a humid chamber. After 3x5 min wash in PBS slides were mounted in Tris-buffered glycerol containing n-propyl gallate[32] with coverslips and were sealed with nail polish. Imaging was carried out using a Leica SP5 confocal microscope equipped with a 405 nm blue diode and argon and helium neon lasers and oil immersion lenses.

*EH-myomesin expression Westernblot*

Following SDS-PAGE on a 4-8% TruPAGE Precast Gel (Sigma) at 120V, the human heart tissue samples were transferred overnight onto nitrocellulose (GE Healthcare Amersham) using a Bio-Rad Wet Blot system at 55 mA. Transfer was visualised with Ponceau Red, followed by blocking in 5% non-fat dry milk (Sainsbury's) in Low Salt Buffer for one hour. After incubation with primary antibody against human EH-myomesin[32] and secondary antibody (HRP-conjugated goat anti rabbit immunoglobulins; Calbiochem), the chemiluminescence signal was

visualised using Clarity Western ECL Substrate (Bio-Rad) and detected with a Bio-Rad ChemiDoc Gel Imaging System. For quantification, blots were reprobed with a polyclonal antibody against all actin isoforms (Sigma) and densitometry was carried out using a Mathematica algorithm generously provided by Dr Mark Holt (Randall Division, King's College London).

*Statistics*

Graphpad Prism software was used for statistical analysis. $F_{max}$ of patient cardiomyocytes was compared to control cardiomyocytes with one-way ANOVA. $Ca^{2+}$-sensitivity was calculated as $EC_{50}$ and length-dependent activation as $\Delta EC_{50}$. The amount of fibrosis, $EC_{50}$, $\Delta EC_{50}$, N2BA/N2B ratio, phosphorylation of cTnI and glutathionylation of cMyBP-C were compared with one-way ANOVA. Phosphorylation of cMyBP-C was compared between groups with non-parametric Kruskal-Wallis test. $F_{pass}$ in patient cardiomyocytes were compared to control cardiomyocytes by 2-way ANOVA. Correlations between N2BA/N2B and N2BA size, N2BA/N2B and fibrosis and glutathionylation and phosphorylation of cMyBP-C were studied with linear regression. All values are shown as means ± standard errors of the mean. Statistical analysis was performed with Graphpad Prism v7. A p-value<0.05 was considered to represent a significant difference and is indicated with * in figures.

**Results**

*High $F_{pass}$ and blunted length-dependent activation of PPCM myofilaments*

The 16 control samples used for experiments were derived from 7 females and 9 males with an age of 44.1±2.9 years, the PPCM samples of 6 females with an age of 35.7±3.2 years, the DCM samples from 3 females and 5 males with an age of 50.0±2.9 and the ISHD samples from 4 males with an age of 56.0±2.7.To establish changes in functional remodeling of cardiomyocytes, myofilament force measurements were performed in membrane-permeabilized cardiomyocytes. $F_{max}$ was similar in all groups (Figure 1A), while $F_{pass}$ was significantly higher in PPCM samples compared to DCM, ISHD and controls (Figure 1B). $Ca^{2+}$-sensitivity of myofilaments was significantly higher in all patient groups compared to controls, evident from the leftward shift of the Force-$Ca^{2+}$ relationship (Figure 1C) and significantly lower $EC_{50}$ in PPCM, DCM and ISHD samples compared to controls (Figure 1D). Length-dependent activation of myofilaments, indicated by the slope of the curve in Figure 1E, was lower in PPCM and DCM samples, but not in ISHD samples compared to controls. The drop in length-dependent

activation, expressed as $\Delta EC_{50}$, was largest in PPCM samples and significantly different from controls (Figure 1F).

*More compliant titin and fibrosis in PPCM and DCM but not in ISHD*

Titin is a giant sarcomeric protein that spans the entire sarcomere from the Z-disk to the M-band and is important in the regulation of $F_{pass}$ through isoform switching and phosphorylation[33]. In addition, it has been suggested that a switch to the more compliant titin isoform leads to reduced LDA[34, 35]. Titin can exist in the small and stiff N2B isoform, and longer and more compliant N2BA isoforms. It is has been shown that changes in titin isoform composition and phosphorylation contribute to DCM pathogenesis[36, 37]. However, it is unknown if titin isoform composition and phosphorylation is altered in PPCM patients. Titin isoforms were separated with gel electrophoresis (Figure 2A). While PPCM samples showed a non-significant and DCM samples a significant increase in N2BA/N2B ratio compared to controls, ISHD samples did not differ from controls (Figure 2B). The size of N2BA titin was also increased in PPCM and DCM samples, while a smaller increase in N2BA size was observed in ISHD samples compared to controls (Figure 2C). The size of the N2BA titin isoforms significantly correlated with the N2BA/N2B ratio in DCM and PPCM samples, but not in ISHD and controls (Figure 2D). This implies that there is not only more N2BA titin, but also larger N2BA isoforms in PPCM and DCM samples.

The increase in titin size and N2BA/N2B ratio implies that the heart induces a response to increase cellular compliance, possibly in response to stiffening of the heart by fibrosis. We therefore measured the amount of fibrosis by picro-Sirius red staining in the same tissue samples in which N2BA/N2B ratio and titin size were measured. Figure 2E shows representative pictures of tissue samples in which fibrosis is stained in fierce red. A significant increase in fibrosis was found in PPCM and DCM samples compared to controls (Figure 2F), while the increase in fibrosis observed in ISHD samples was not significant compared to controls (Figure 2F). Figure 2G illustrates that a higher level of fibrosis coincides with higher N2BA/N2B ratios in PPCM and DCM samples.

*Reduced phosphorylation and preserved glutathionylation of cMyBP-C in end-stage dilated cardiomyopathies*

Oxidative stress has been shown to play an important role in PPCM pathogenesis and is also reported in other forms of heart failure[7, 38], and may underlie the changes in cellular function. Oxidative stress can cause glutathionylation of various proteins and thereby alter their function[39, 40]. Glutathionylation of cMyBP-C has

been shown to impair phosphorylation of cMyBP-C and subsequently decelerate $Ca^{2+}$- mediated force kinetics in DCM and ISHD[40]. ProQ-stained (Figure 3A, upper panel; phosphorylation) and SYPRO-stained (Figure 3A, lower panel; total protein) gel analysis showed decreased phosphorylation of cMyBP-C (Figure 3B) in PPCM, DCM and ISHD compared to controls. Western blots for glutathionylated proteins (Figure 3C upper panel glutathionylated cMyBP-C and Figure 3C lower panel total cMyBP-C) showed there was no significant increase in glutathionylated cMyBP-C (Figure 3D) in PPCM, DCM and ISHD samples compared to controls. Also no correlation was found between the amount of glutathionylated cMyBP-C and phosphorylation of cMyBP-C (Figure 3E). This implies that the decreased phosphorylation of cMyBP-C in these samples was not caused by glutathionylation of cMyBP-C. The decreased phosphorylation of cMyBP-C could have been caused by desensitization of the β-adrenergic receptors and subsequent impaired PKA-mediated phosphorylation, a mechanism confirmed in various forms of heart failure[41].

*Restoration of cTnI and titin phosphorylation normalized $F_{pass}$, $Ca^{2+}$-sensitivity and length- dependent activation of myofilaments*

Decreased PKA-mediated phosphorylation at Ser4010 of titin could underlie the higher $F_{pass}$ in PPCM[42]. Phosphorylation of Ser4010 was indeed decreased in PPCM samples compared to controls (Figure 4A,C). However, Ser4010 phosphorylation was also decreased in DCM (Figure 4A,C), while $F_{pass}$ was not altered in DCM samples. An alternative hypothesis for the discrepant change in $F_{pass}$ in PPCM and DCM would be that PKC-mediated phosphorylation of titin is increased in PPCM leading to an increased $F_{pass}$ [42]. However, PKC-mediated phosphorylation at Ser12022 was decreased rather than increased in PPCM, and unaltered in DCM and ISHD compared to controls (Figure 2B,D). In order to determine if the decrease in Ser4010 phosphorylation was causal to the increase in $F_{pass}$ in PPCM samples we repeated the experiments after incubation with exogenous PKA. Indeed, PKA normalized $F_{pass}$ in PPCM samples (Figure 4E). Impaired PKA-mediated phosphorylation could also cause hypophosphorylation of cTnI, which is an important regulator of myofilament $Ca^{2+}$-sensitivity and length-dependent activation[43, 44]. Indeed, cTnI phosphorylation was also decreased in PPCM, DCM and ISHD samples compared to controls (Figure 3A, 4F). A PhosTag analysis of cTnI showed prominent mono- and bis-phosphorylation of cTnI in controls while PPCM and DCM samples showed prominent non- and mono-phosphorylation of cTnI. The ISHD samples showed predominantly mono-phosphorylated cTnI (Figure 4G,H). Exogenous PKA normalized myofilament $Ca^{2+}$-sensitivity in PPCM, DCM and ISHD samples to

control levels (Figure 4I,J). In addition, exogenous PKA restored $\Delta EC_{50}$ in PPCM and DCM to control levels (Figure 4K).

*Expression of EH-myomesin in DCM but not in PPCM and ISHD samples*

Although $F_{pass}$ normalized to control levels after PKA in the PPCM samples, we set out to find an explanation for the discrepant finding of $F_{pass}$ and titin phosphorylation in PPCM, DCM and ISHD samples. Myomesin is a component of the M-band and is important for sarcomere stability. The fetal form of myomesin, EH-myomesin, has been shown to be a hallmark of DCM and is virtually absent in adult healthy heart tissue[32]. It is believed that EH-myomesin is re-expressed in order to provide stability in overstretched conditions in DCM. Our study confirmed EH-myomesin was re-expressed in DCM samples (Figure 5C,G). Expression of EH-myomesin was much lower in ISHD samples (Figure 5D,H) and almost absent in PPCM samples (Figure 5B,F). Our control patients did not show expression of EH-myomesin or only at a very low level (Figure 5A,E). Western blot analysis confirmed high EH-myomesin expression in DCM, but not in PPCM and controls (Figure 5I, J). Thus, the increase in titin N2BA/N2B ratio is accompanied by an increase in EH-myomesin in DCM, but not in PPCM. The absence of the stabilizing effect of EH-myomesin expression in PPCM may provide an explanation why PPCM showed more impairment of myofilament function compared to DCM, while titin isoform expression and PKA-mediated myofilament phosphorylation were similar in the two groups.

**Discussion**

The clinical similarities and differences in disease onset, progression and outcome between PPCM and DCM patients suggest that the cellular pathomechanisms overlap, but may also show distinct changes. Here, we show that myofilament function is more impaired in PPCM compared to DCM with respect to length-dependent activation and $F_{pass}$. In addition, myofilament remodeling was different, since DCM samples expressed EH-myomesin, while PPCM samples did not. On the other hand, PPCM and DCM samples showed similar changes in myofilament $Ca^{2+}$-sensitivity and sarcomeric protein phosphorylation.

*Fibrosis content is higher in PPCM and DCM compared to ISHD and controls*

While fibrosis is consistently reported in DCM, [45, 46] , reports on the occurrence of fibrosis in PPCM patients are conflicting[47-50] while animal models of PPCM show fibrosis[51]. MRI data at diagnosis of PPCM in patients display

frequently no hint for fibrosis, a feature that would be consistent with the ability of many patients to fully recover from the disease[17, 52]. In the present study, we found fibrosis in both DCM and PPCM samples. However, it must be noted that the assessment of fibrosis was performed in small tissue areas of samples obtained during heart transplantation. It cannot be excluded that the tissue samples were selectively taken from more fibrotic regions and may thus not be representative for whole heart fibrosis content. Techniques such as magnetic resonance imaging (MRI) might give a better impression of whole heart fibrosis content. No late gadolinium enhancement by MRI was shown in PPCM (2 acute phase patients and 4 patients at a later stage) previously[49]. In addition, our fibrosis analysis was only performed in end-stage explanted heart tissue of PPCM patients and might therefore have been induced over time and may not reflect the acute or short term PPCM situation. The ISHD samples were taken from the remote area and not within the infarct zone. While PPCM and DCM are more likely to show a diffuse fibrosis pattern and therefore any part of the heart taken might show fibrosis, the fibrosis in ISHD is more likely to be localized in or close to the infarct area. This could explain why we found very little fibrosis in the ISHD samples.

*PKA-mediated hypophosphorylation in all dilated cardiomyopathies*

Independent of the initial cause, all forms of dilated cardiomyopathy (PPCM, DCM and ISHD) exhibited higher myofilament $Ca^{2+}$-sensitivity compared to controls, while only PPCM samples had an increased $F_{pass}$. The increase in myofilament $Ca^{2+}$-sensitivity was attributed to decreased PKA-mediated phosphorylation of cTnI since incubation with exogenous PKA restored $Ca^{2+}$-sensitivity to controls in all groups. The increased $F_{pass}$ in PPCM samples was also restored with exogenous PKA and a decreased PKA-mediated phosphorylation of titin was confirmed at Ser4010. In addition, we also found a decreased phosphorylation of cMyBP-C which was not related to glutathionylation of cMyBP-C. These combined results strengthen the suggestion that PKA-mediated phosphorylation was impaired in all heart failure samples. The β-adrenergic receptors were shown to be desensitized leading to impaired PKA-mediated phosphorylation of sarcomeric proteins in various forms of heart failure[41] and we have now confirmed PKA-mediated phosphorylation is impaired in end-stage PPCM as well. Despite a similar downregulation of cTnI phosphorylation, the $\Delta EC_{50}$ was significantly decreased only in PPCM samples compared to controls. While DCM samples showed a non-significant impairment of length-dependent activation, ISHD samples had normal length-dependent activation values compared to controls despite their increased $Ca^{2+}$-sensitivity. A decreased length-dependent activation has been reported for

samples with compliant titin[35, 53], and an increase in compliant titin has been reported in DCM[36, 37]. We observed an increase in N2BA/N2B ratio in PPCM and DCM samples compared to controls. In addition, an increase in size of the compliant titin isoform was found corresponded to 58 kDa in PPCM, 93 kDa in DCM and 48 kDa in ISHD samples compared to controls. Although this increase was not significant, it is of a magnitude that should not be ignored since such an increase in molecular weight might alter protein function. The fact that titin N2BA size and N2BA/N2B ratio were significantly correlated in DCM and PPCM samples indicates that the same regulatory mechanism is responsible for both the shift in isoform and the inclusion of additional exons to make N2BA bigger. This observation is in line with the increase in titin N2BA size and N2BA/N2B ratio found in a patient with a mutation in RBM20[24]. The observation that in ISHD N2BA size was increased, while N2BA/N2B ratio was unaltered implies the isoform shift is preceded by inclusion of additional exons in N2BA after which both titin size and N2BA expression increase further. Both cTnI phosphorylation as well as titin isoform composition are regulators of myofilament length-dependent activation[34]. The decreased cTnI phosphorylation and increase in N2BA/N2B and N2BA size explain the blunted myofilament length- dependent activation in PPCM and DCM samples. The preserved myofilament length-dependent activation in ISHD samples, which showed decreased cTnI phosphorylation and unaltered N2BA/N2B ratio, indicates a synergistic role of cTnI phosphorylation and titin in regulating myofilament length-dependent activation.

*Different myofilament remodeling of the M-band in PPCM and DCM*

PPCM and DCM samples both had decreased phosphorylation at Ser4010 of titin and a similar increase in N2BA/N2B ratio, while $F_{pass}$ was higher compared to controls only in PPCM. The expression of myomesin isoforms follows the expression of titin isoforms in various muscle types. The longer compliant isoforms of titin and EH-myomesin are predominantly expressed in the fetal heart and are replaced by the shorter and stiffer myomesin during the progression to adulthood[54, 55]. This was also reported for soleus where the larger titin N2A isoform[56] is expressed, the EH-myomesin dominates[57]. The re-expression of EH-myomesin in DCM patients could be a result of the induction of the fetal gene program which has been shown in various forms of heart failure and is believed to be activated in order to cope with the changes in cardiac demand[58]. Whether the expression of these fetal genes is beneficial is still under debate. EH-myomesin acts as a mini-spring and has an additional domain of approximately 200 amino acids, similar to the PEVK domain of titin[59]. It is believed that EH-myomesin provides stability to the sarcomere in overstretched conditions[59]. Here we presented evidence

that expression of EH-myomesin might prevent an increase in $F_{pass}$ and decrease of length- dependent activation in DCM patients, but not in PPCM patients who do not express EH-myomesin. Exogenous PKA restored $F_{pass}$ and length- dependent activation in PPCM samples indicating that the lack of EH-myomesin is overcome by PKA-mediated protein phosphorylation. An in vitro study showed phosphorylation of myomesin at Ser-482 by PKA and subsequent disturbance of the interaction between titin (through M4 domain) and myomesin (My4-My6 domains)[60]. However, Fukuzawa et al. could not confirm titin (M4)-myomesin (My4-My6) interaction in a pulldown assay or forced yeast two hybrid assay. In addition, phosphorylation of myomesin did not affect myomesin-obscurin interaction[61]. Therefore, the effect of myomesin phosphorylation in vivo warrants further research. Nonetheless, in heart failure where the β-adrenergic receptors are desensitized and PKA-mediated phosphorylation of sarcomeric proteins such as cTnI and titin is decreased, the expression of EH-myomesin may play an important role in stabilization of the sarcomeres in order to maintain or limit the increase in $F_{pass}$ and impairment of length-dependent activation.

*Clinical perspective*

Although PPCM and DCM have similar clinical phenotypes, they differ in their clinical progression and therefore have a different prognosis. We show here that myofilament remodeling is different in PPCM and DCM. We also show that PPCM samples suffer from impaired PKA-mediated phosphorylation similar to what has been observed in DCM samples, but that the effect on myofilament function is larger in PPCM. These observations could provide a possible explanation why PPCM patients have such a strong response to stimulation of their β-adrenergic system[20]. The notion that we could restore all parameters with exogenous PKA indicates that both PPCM and DCM patients might benefit from an increase in β-adrenergic stimulation in order to normalize myofilament function. However we have discussed before that dobutamine, a β-adrenergic receptor agonist, worsens heart failure in PPCM patients and STAT3 KO mice, and is associated with adverse outcome independent of treatment with bromocriptine[13, 20]. These results question whether the β-adrenergic system is therefore a realistic clinical target in PPCM treatment. However, increasing $Ca^{2+}$-sensitivity has been a target for the treatment of systolic dysfunction since a greater force is generated at lower calcium concentrations in order to achieve sufficient contractile power in systolic dysfunction. We show that the myofilaments are already very $Ca^{2+}$ sensitive and this should be taken into consideration when considering high $Ca^{2+}$-sensitivity

might impair . In addition, too length-dependent activation high $Ca^{2+}$-sensitivity might cause contraction at diastolic calcium concentrations and thereby contributes to cardiac dysfunction.

*Conclusion*

We show that different forms of heart failure; PPCM, DCM and ISHD, share aspects of underlying pathomechanisms but they also differ in important aspects. An overview of the changes in each form of heart failure is shown in Figure 6. PPCM, DCM and ISHD have decreased cMyBP-C phosphorylation and increased $Ca^{2+}$-sensitivity induced by decreased phosphorylation of cTnI. However, PPCM and DCM share additional pathomechanisms such as increased compliant titin, reduced phosphorylation of titin at Ser4010 and impaired myofilament length-dependent activation, observations that were not seen in ISHD. The increase in myofilament $Ca^{2+}$-sensitivity and decreased length-dependent activation was more pronounced in PPCM samples. Both parameters could be restored after incubation with exogenous PKA. In addition, DCM but not PPCM patients show induction of the expression of EH-myomesin. The lack of EH-myomesin re-expression might have contributed to an increase in $F_{pass}$ and severely blunted length- dependent activation in PPCM patients in situations of low PKA-mediated phosphorylation due to instability of the sarcomeres in overstretched conditions. Therefore, this study shows myofilament remodeling and function is more impaired in PPCM compared to DCM and ISHD, and the lack of EH-myomesin re-expression may explain the fast deterioration of some PPCM patients to end-stage heart failure.

**Limitation to the study**

No tissue from healthy postpartum women could be explored and therefore the condition of a healthy maternal heart in the postpartum phase is not known. In addition, the different heart failure groups could not be completely matched regarding age and gender of patient samples studied. However, no difference was observed between samples derived from males and females in the DCM group.

**Acknowledgements**

We would like to thank Ruud Zaremba, Max Goebel, Wies Lommen and Sabine Bongardt for technical assistance. We thank the Sydney Heart Bank for the samples used in this study. We are grateful to Dr Mark Holt (Randall Division, King's College London) for help with densitometry.

**Funding**

We acknowledge the support from the Netherlands Cardiovascular Research Initiative, an initiative with support of the Dutch Heart Foundation, CVON2011-11 ARENA and Rembrandt Institute for Cardiovascular Sciences 2013. EE and KF are supported by the British Heart Foundation. FWA is supported by a Dekker scholarship-Junior Staff Member 2014T001 of the Dutch Heart Foundation and UCL Hospitals NIHR Biomedical Research Centre.

**Figure legends**

**Figure 1. Baseline characteristics**

**A:** $F_{max}$ was not significantly different in PPCM (25.1±2.3 kN/$m^2$, N=4, n=16), DCM (27.9±1.7 kN/$m^2$, N=6, n=27) and ISHD (30.9±1.9 kN/$m^2$, N=4, n=15) compared to controls (29.7±1.8 kN/$m^2$, N=7, n=30). **B:** $F_{pass}$ was significantly increased in PPCM (N=4, n=14, p<0.0001) compared to controls (N=7, n=18). $F_{pass}$ was not significantly altered in DCM (N=6, n=15) and ISHD (N=4, n=9) compared to controls. **C:** The force-calcium curve was shifted to the left compared in PPCM (N=4, n=8), DCM (N=6, n=13) and ISHD (N=4, n=6) samples compared to controls (N=7, n=17). **D:** $Ca^{2+}$-sensitivity, measured as $EC_{50}$, was significantly increased in PPCM (1.19±0.08 µM, N=4, n=8, p<0.0001), DCM (1.27±0.08 µM, N=6, n=13, p<0.0001) and ISHD (1.25±0.10 µM, N=4, n=6, p<0.0001) compared to controls (1.84 ±0.05 µM, N=7, n=17). **E:** Length-dependent activation, indicated by the increase in $Ca^{2+}$-sensitivity upon stretch, was decreased in PPCM and DCM, but not in ISHD compared to controls. **F:** The shift in $Ca^{2+}$-sensitivity, indicated by $\Delta EC_{50}$ was significantly reduced in PPCM (0.26±0.05 µM, N=4, n=8, p=0.0234) compared to controls (0.54 ±0.08 µM, N=7, n=17), while it was non-significantly reduced in DCM (0.41±0.03 µM, N=6, n=13) and similar to controls in ISHD (0.52±0.06 µM, N=4, n=6).

**Figure 2: Titin isoform shift in DCM and PPCM and fibrosis in all dilated cardiomyopathies**

**A:** Titin isoforms N2BA and N2B were separated with gel electrophoresis. **B:** N2BA/N2B was increased in DCM (0.84±0.16, N=8, p=0.0327) and non-significantly in PPCM (0.82±0.15, N=6), but not in ISHD (0.43±0.07, N=4) compared to controls (0.52±0.02, N=15). **C:** The size of N2BA titin was non-significantly increased in DCM (3471±39 kDa, N=8) and PPCM (3446±39 kDa, N=5) compared to controls (3388±16 kDa, N=9) while a smaller

increase in N2BA size was observed in ISHD (3436±7 kDa, N=4). **D:** The size of N2BA was significantly correlated to the N2BA/N2B ratio in PPCM (p=0.0479, $R^2$=0.7775) and DCM (p=0.0365, $R^2$=0.5450), but not in ISHD, controls or all groups combined. **E:** Representative pictures of cryosections stained with picro-Sirius red of a control, PPCM, DCM and ISHD sample. **F:** Fibrosis was significantly increased in PPCM (4.51±0.66%, N=4, p=0.0003) and DCM (5.46±0.55%, N=8, p<0.0001) compared to controls (1.21±0.23%, N=9), while fibrosis was only non-significantly increased in ISHD (2.92±0.46%, N=4). **G:** No significant correlation was found between the amount of fibrosis and N2BA/N2B.

**Figure 3: Glutathionylation and phosphorylation of MyBP-C**

**A:** Upper panel: gel stained with ProQ diamond. Lower panel: same gel stained with SYPRO Ruby. **B:** Phosphorylation of cMyBP-C was significantly decreased in PPCM (N=5, p=0.0125), DCM (N=6 p=0.0027) and ISHD (N=4, p=0.0011) compared to controls (N=13). **C:** Representative blots stained with α-glutathione (upper panel), cMyBP-C (lower panel). **D:** Glutathionylation of cMyBP-C was not different in PPCM (N=4), DCM (N=4) and ISHD (N=3) compared to controls (N=11). **E:** No correlation was found between gluthationylation and phosphorylation of cMyBP-C.

**Figure 4: Impaired β-adrenergic signaling in PPCM, DCM and ISHD**

**A**: Representative pictures of phosphorylated titin at Ser4010 (upper panel) and total titin (lower panel). **B**: Representative pictures of phosphorylated titin at Ser12022 (upper panel) and total titin (lower panel). **C:** PKA-mediated phosphorylation of titin at Ser4010 was significantly reduced in PPCM (N=5, p=0.0140) and DCM samples (N=6, p=0.0051) compared to controls (N=12) while it was not altered in ISHD samples (N=4). **D:** PKC mediated phosphorylation of titin at Ser12022 was non-significantly decreased in PPCM (N=4) but normal in DCM (N=6) and ISHD (N=3) samples compared to controls (N=11). **E:** $F_{pass}$ normalized to controls (N=7, n=14) after incubation with exogenous PKA in PPCM samples (N=4, n=11), while it did not alter $F_{pass}$ in DCM (N=6, n=11) or ISHD (N=4, n=10) samples. **F**: Phosphorylation of cTnI was significantly reduced in PPCM (N=5, p=0.0004) and DCM (N=6, p=0.001) and non-significantly in ISHD (N=4, p=0.0681) samples compared to controls (N=13). **G:** PhosTag analysis showed separation of non-, mono- and bis- phosphorylation of cTnI. **H**: PhosTag analysis showed predominantly mono-and bisphosphorylation of cTnI in controls (N=8) while non- and mono-phosphorylation was more prevalent in PPCM (N=5) and DCM (N=6). ISHD samples (N=3) showed mostly

mono-phosphorylation of cTnI. **I:** Incubation with exogenous PKA normalized $Ca^{2+}$-sensitivity in PPCM (1.79±0.12, N=5 n=8), DCM (2.02±0.09, N=6, n=8) and ISHD (2.01±0.15, N=4, n=6) samples compared to controls (1.81±0.06, N=6, n=17). **J:** Length-dependent activation, indicated by the increase in $Ca^{2+}$-sensitivity upon stretch, was normalized after incubation with exogenous PKA to controls in PPCM (N=5 n=8), DCM (N=6, n=8) and ISHD (N=4, n=6) samples compared to controls (N=6, n=17). **K**: The shift in $Ca^{2+}$-sensitivity upon stretch, indicated by $\Delta EC_{50}$ was normalized to controls after incubation with exogenous PKA in PPCM (0.51±0.09, N=5 n=8), DCM (0.58±0.08, N=6, n=8) and ISHD (0.63±0.11, N=4, n=6) samples compared to controls (0.53±0.07, N=6, n=17).

**Figure 5: EH-myomesin expression in DCM, but only limited in PPCM and ISHD compared to controls**

Representative immunohistochemical pictures of controls (**A**), PPCM (**B**), DCM (**C**) and ISHD (**D**) in which EH-myomesin is stained in green, all myomesin isoforms in red and nuclei in blue. The percentage of patients in control (**E**), PPCM (**F**), DCM (**G**) and ISHD (**H**) groups that fall in various categories of degree of EH-myomesin expression is indicated in pie charts. **I:** Western blot showed EH-myomesin expression (upper panel) relative to actin (lower panel) is non-significantly increased in DCM (N=4) compared to PPCM (N=4) and controls (N=2) (**J**).

**Figure 6: Overview of pathological changes in PPCM, DCM and ISHD**

All dilated cardiomyopathies showed a decreased cMyBP-C phosphorylation and an increase in $Ca^{2+}$-sensitivity induced by decreased phosphorylation of cTnI. However, PPCM and DCM share additional pathomechanisms such as increased compliant titin, reduced phosphorylation of titin at Ser4010 and impaired length-dependent activation. Phosphorylation of titin Ser-12022 was only decreased in PPCM. While DCM samples showed re-expression of EH-myomesin, PPCM and ISHD samples did not. The lack of EH-myomesin re-expression in PPCM in combination with low cTnI phosphorylation and enhanced compliant titin isoform expression may explain high $F_{pass}$ and the more pronounced myofilament length-dependent activation impairment in PPCM.

**References**

[1] Elliott P, Andersson B, Arbustini E, Bilinska Z, Cecchi F, Charron P, Dubourg O, Kuhl U, Maisch B, McKenna WJ, Monserrat L, Pankuweit S, Rapezzi C, Seferovic P, Tavazzi L, Keren A: Classification of the cardiomyopathies: a position statement from the European Society Of Cardiology Working Group on Myocardial and Pericardial Diseases. Eur Heart J 2008, 29:270-6.

[2] Pearson GD, Veille J-C, Rahimtoola S, Hsia J, Oakley CM, Hosenpud JD, Ansari A, Baughman KL: Peripartum Cardiomyopathy National Heart, Lung, and Blood Institute and Office of Rare Diseases (National Institutes of Health) Workshop Recommendations and Review. JAMA 2000, 283:1183-8.

[3] Ware JS, Li J, Mazaika E, Yasso CM, DeSouza T, Cappola TP, Tsai EJ, Hilfiker-Kleiner D, Kamiya CA, Mazzarotto F, Cook SA, Halder I, Prasad SK, Pisarcik J, Hanley-Yanez K, Alharethi R, Damp J, Hsich E, Elkayam U, Sheppard R, Kealey A, Alexis J, Ramani G, Safirstein J, Boehmer J, Pauly DF, Wittstein IS, Thohan V, Zucker MJ, Liu P, Gorcsan J, 3rd, McNamara DM, Seidman CE, Seidman JG, Arany Z, Imac, Investigators I: Shared Genetic Predisposition in Peripartum and Dilated Cardiomyopathies. N Engl J Med 2016, 374:233-41.

[4] van Spaendonck-Zwarts KY, Posafalvi A, van den Berg MP, Hilfiker-Kleiner D, Bollen IA, Sliwa K, Alders M, Almomani R, van Langen IM, van der Meer P, Sinke RJ, van der Velden J, Van Veldhuisen DJ, van Tintelen JP, Jongbloed JD: Titin gene mutations are common in families with both peripartum cardiomyopathy and dilated cardiomyopathy. Eur Heart J 2014, 35:2165-73.

[5] van Spaendonck-Zwarts KY, van Tintelen JP, van Veldhuisen DJ, van der Werf R, Jongbloed JD, Paulus WJ, Dooijes D, van den Berg MP: Peripartum cardiomyopathy as a part of familial dilated cardiomyopathy. Circulation 2010, 121:2169-75.

[6] Hershberger RE, Hedges DJ, Morales A: Dilated cardiomyopathy: the complexity of a diverse genetic architecture. Nat Rev Cardiol 2013, 10:531-47.

[7] Hilfiker-Kleiner D, Kaminski K, Podewski E, Bonda T, Schaefer A, Sliwa K, Forster O, Quint A, Landmesser U, Doerries C, Luchtefeld M, Poli V, Schneider MD, Balligand JL, Desjardins F, Ansari A,

Struman I, Nguyen NQ, Zschemisch NH, Klein G, Heusch G, Schulz R, Hilfiker A, Drexler H: A cathepsin D-cleaved 16 kDa form of prolactin mediates postpartum cardiomyopathy. Cell 2007, 128:589-600.

[8] Sliwa K, Blauwet L, Tibazarwa K, Libhaber E, Smedema JP, Becker A, McMurray J, Yamac H, Labidi S, Struman I, Hilfiker-Kleiner D: Evaluation of bromocriptine in the treatment of acute severe peripartum cardiomyopathy: a proof-of-concept pilot study. Circ 2010, 121:1465-73.

[9] Fett JD: Peripartum cardiomyopathy: A puzzle closer to solution. World J Cardiol 2014, 6:87-99.

[10] Elkayam U: Clinical characteristics of peripartum cardiomyopathy in the United States: diagnosis, prognosis, and management. J Am Coll Cardiol 2011, 58:659-70.

[11] Felker GM, Thompson RE, Hare JM, Hruban RH, Clemetson DE, Howard DL, Baughman KL, Kasper EK: Underlying causes and long- term survival in patients with initially unexplained cardiomyopathy. N Engl J Med 2000, 342:1077-84.

[12] Ballo P, Betti I, Mangialavori G, Chiodi L, Rapisardi G, Zuppiroli A: Peripartum cardiomyopathy presenting with predominant left ventricular diastolic dysfunction: efficacy of bromocriptine. Case Rep Med 2012, 2012:476903.

[13] Haghikia A, Podewski E, Libhaber E, Labidi S, Fischer D, Roentgen P, Tsikas D, Jordan J, Lichtinghagen R, von Kaisenberg CS, Struman I, Bovy N, Sliwa K, Bauersachs J, Hilfiker-Kleiner D: Phenotyping and outcome on contemporary management in a German cohort of patients with peripartum cardiomyopathy. Basic Res Cardiol 2013, 108:366.

[14] van Hoeven KH, Kitsis RN, Katz SD, Factor SM: Peripartum versus idiopathic dilated cardiomyopathy in young women - a comparison of clinical, pathologic and prognostic features. Int J Cardiol 1993, 40:57-65.

[15] Goland S, Modi K, Bitar F, Janmohamed M, Mirocha JM, Czer LS, Illum S, Hatamizadeh P, Elkayam U: Clinical profile and predictors of complications in peripartum cardiomyopathy. J Card Fail 2009, 15:645-50.

[16] Grewal J, Siu SC, Ross HJ, Mason J, Balint OH, Sermer M, Colman JM, Silversides CK: Pregnancy outcomes in women with dilated cardiomyopathy. J Am Coll Cardiol 2009, 55:45-52.

[17] Hilfiker-Kleiner D, Sliwa K: Pathophysiology and epidemiology of peripartum cardiomyopathy. Nat Rev Cardiol 2014, 11:364-70.

[18] Patten IS, Rana S, Shahul S, Rowe GC, Jang C, Liu L, Hacker MR, Rhee JS, Mitchell J, Mahmood F, Hess P, Farrell C, Koulisis N, Khankin EV, Burke SD, Tudorache I, Bauersachs J, del Monte F, Hilfiker-Kleiner D, Karumanchi SA, Arany Z: Cardiac angiogenic imbalance leads to peripartum cardiomyopathy. Nature 2012, 485:333-8.

[19] Grattan DR, Steyn FJ, Kokay IC, Anderson GM, Bunn SJ: Pregnancy-induced adaptation in the neuroendocrine control of prolactin secretion. J Neuroendocrinol 2008, 20:497-507.

[20] Stapel B, Kohlhaas M, Ricke-Hoch M, Haghikia A, Erschow S, Knuuti J, Silvola JM, Roivainen A, Saraste A, Nickel AG, Saar JA, Sieve I, Pietzsch S, Muller M, Bogeski I, Kappl R, Jauhiainen M, Thackeray JT, Scherr M, Bengel FM, Hagl C, Tudorache I, Bauersachs J, Maack C, Hilfiker-Kleiner D: Low STAT3 expression sensitizes to toxic effects of beta-adrenergic receptor stimulation in peripartum cardiomyopathy. Eur Heart J 2016.

[21] van Dijk SJ, Paalberends ER, Najafi A, Michels M, Sadayappan S, Carrier L, Boontje NM, Kuster DW, van Slegtenhorst M, Dooijes D, dos Remedios C, ten Cate FJ, Stienen GJ, van der Velden J: Contractile dysfunction irrespective of the mutant protein in human hypertrophic cardiomyopathy with normal systolic function. Circ Heart Fail 2012, 5:36-46.

[22] van der Velden J, de Jong J, Owen VJ, Burton PB, Stienen GJ: Effect of protein kinase A on calcium sensitivity of force and its sarcomere length dependence in human cardiomyocytes. Cardiovasc Res 2000, 46:487-95.

[23] Warren CM, Krzesinski PR, Greaser ML: Vertical agarose gel electrophoresis and electroblotting of high-molecular-weight proteins. Electrophoresis 2003, 24:1695-702.

[24] Beqqali A, Bollen IA, Rasmussen TB, van den Hoogenhof MM, van Deutekom HW, Schafer S, Haas J, Meder B, Sorensen KE, van Oort RJ, Mogensen J, Hubner N, Creemers EE, van der Velden J, Pinto YM: A mutation in the glutamate-rich region of RNA-binding motif protein 20 causes dilated

cardiomyopathy through missplicing of titin and impaired Frank-Starling mechanism. Cardiovasc Res 2016, 112:452-63.

[25] Ottenheijm CA, Knottnerus AM, Buck D, Luo X, Greer K, Hoying A, Labeit S, Granzier H: Tuning passive mechanics through differential splicing of titin during skeletal muscle development. Biophys J 2009, 97:2277-86.

[26] Kötter S, Kazmierowska M, Andresen C, Bottermann K, Grandoch M, Gorressen S, Heinen A, Moll JM, Scheller J, Gödecke A, Fischer JW, Schmitt JP, Krüger M: Titin-Based Cardiac Myocyte Stiffening Contributes to Early Adaptive Ventricular Remodeling After Myocardial Infarction. Circ Res 2016, 119.

[27] Zaremba R, Merkus D, Hamdani N, Lamers JM, Paulus WJ, Dos Remedios C, Duncker DJ, Stienen GJ, van der Velden J: Quantitative analysis of myofilament protein phosphorylation in small cardiac biopsies. Proteomics Clin Appl 2007, 1:1285-90.

[28] Najafi A, Schlossarek S, van Deel ED, van den Heuvel N, Guclu A, Goebel M, Kuster DW, Carrier L, van der Velden J: Sexual dimorphic response to exercise in hypertrophic cardiomyopathy-associated MYBPC3-targeted knock-in mice. Pflugers Arch 2015, 467:1303-17.

[29] Avner BS, Shioura KM, Scruggs SB, Grachoff M, Geenen DL, Helseth DL, Jr., Farjah M, Goldspink PH, Solaro RJ: Myocardial infarction in mice alters sarcomeric function via post-translational protein modification. Mol Cell Biochem 2012, 363:203-15.

[30] Kaestner L, Scholz A, Hammer K, Vecerdea A, Ruppenthal S, Lipp P: Isolation and genetic manipulation of adult cardiac myocytes for confocal imaging. J Vis Exp 2009, Video article.

[31] Grove BK, Kurer V, Lehner C, Doetschman TC, Perriard JC, Eppenberger HM: A new 185,000-dalton skeletal muscle protein detected by monoclonal antibodies. J Cell Biol 1984, 98:518-24.

[32] Schoenauer R, Emmert MY, Felley A, Ehler E, Brokopp C, Weber B, Nemir M, Faggian GG, Pedrazzini T, Falk V, Hoerstrup SP, Agarkova I: EH-myomesin splice isoform is a novel marker for dilated cardiomyopathy. Basic Res Cardiol 2011, 106:233-47.

[33] Granzier H, Labeit S: Cardiac titin: an adjustable multi-functional spring. J Physiol 2002, 541:335-42.

[34] Fukuda N, T. T, Ohtsuki I, Ishiwata S, Kurihara S: Titin and troponin: central players in the frank-starling mechanism of the heart. Curr Cardiol Rev 2009, 5:119-24.

[35] Fukuda N, Wu Y, Farman G, Irving TC, Granzier H: Titin isoform variance and length dependence of activation in skinned bovine cardiac muscle. J Physiol 2003, 553:147-54.

[36] Makarenko I, Opitz CA, Leake MC, Neagoe C, Kulke M, Gwathmey JK, del Monte F, Hajjar RJ, Linke WA: Passive stiffness changes caused by upregulation of compliant titin isoforms in human dilated cardiomyopathy hearts. Circ Res 2004, 95:708-16.

[37] Nagueh SF, Shah G, Wu Y, Torre-Amione G, King NM, Lahmers S, Witt CC, Becker K, Labeit S, Granzier HL: Altered titin expression, myocardial stiffness, and left ventricular function in patients with dilated cardiomyopathy. Circ 2004, 110:155-62.

[38] Seddon M, Looi YH, Shah AM: Oxidative stress and redox signalling in cardiac hypertrophy and heart failure. Heart 2007, 93:903-7.

[39] Alegre-Cebollada J, Kosuri P, Giganti D, Eckels E, Rivas-Pardo JA, Hamdani N, Warren CM, Solaro RJ, Linke WA, Fernandez JM: S-glutathionylation of cryptic cysteines enhances titin elasticity by blocking protein folding. Cell 2014, 156:1235-46.

[40] Stathopoulou K, Wittig I, Heidler J, Piasecki A, Richter F, Diering S, van der Velden J, Buck F, Donzelli S, Schroder E, Wijnker PJ, Voigt N, Dobrev D, Sadayappan S, Eschenhagen T, Carrier L, Eaton P, Cuello F: S-glutathiolation impairs phosphoregulation and function of cardiac myosin-binding protein C in human heart failure. FASEB J 2016.

[41] Harding S, Brown L, Wynne D, Davies C, Poole-Wilson P: Mechanisms of beta adrenoceptor desensitisation in the failing human heart. Cardiovasc Res 1994, 28:1451-60.

[42] Kötter S, Gout L, Von Frieling-Salewsky M, Muller AE, Helling S, Marcus K, Dos Remedios C, Linke WA, Kruger M: Differential changes in titin domain phosphorylation increase myofilament stiffness in failing human hearts. Cardiovasc Res 2013, 99:648-56.

[43] Wijnker PJM, Sequeira V, Foster DB, Li Y, dos Remedios CG, Murphy AM, Stienen GJM, van der Velden J: Length-dependent activation is modulated by cardiac troponin I bisphosphorylation at

Ser23 and Ser24 but not by Thr143 phosphorylation. Am J Physiol Heart Circ Physiol 2014, 306:H1171–H81.

[44] Konhilas JP, Irving TC, Wolska BM, Jweied EE, Martin AF, Solaro RJ, de Tombe PP: Troponin I in the murine myocardium: influence on length-dependent activation and interfilament spacing. J Physiol 2003, 547:951-61.

[45] Assomull RG, Prasad SK, Lyne J, Smith G, Burman ED, Khan M, Sheppard MN, Poole-Wilson PA, Pennell DJ: Cardiovascular magnetic resonance, fibrosis, and prognosis in dilated cardiomyopathy. J Am Coll Cardiol 2006, 48:1977-85.

[46] Herpel E, Pritsch M, Koch A, Dengler TJ, Schirmacher P, Schnabel PA: Interstitial fibrosis in the heart: differences in extracellular matrix proteins and matrix metalloproteinases in end-stage dilated, ischaemic and valvular cardiomyopathy. Histopathology 2006, 48:736-47.

[47] Kawano H, Tsuneto A, Koide Y, Tasaki H, Sueyoshi E, Sakamoto I, Hayashi T: Magnetic Resonance Imaging in a Patient with Peripartum Cardiomyopathy. Intern Med 2008, 47:97-102.

[48] Leurent G, Baruteau AE, Larralde A, Ollivier R, Schleich JM, Boulmier D, Bedossa M, Langella B, Le Breton H: Contribution of cardiac MRI in the comprehension of peripartum cardiomyopathy pathogenesis. Int J Cardiol 2009, 132:e91-3.

[49] Mouquet F, Lions C, de Groote P, Bouabdallaoui N, Willoteaux S, Dagorn J, Deruelle P, Lamblin N, Bauters C, Beregi JP: Characterisation of peripartum cardiomyopathy by cardiac magnetic resonance imaging. Eur Radiol 2008, 18:2765–9.

[50] Ntusi NBA, Chin A: Letter to the editor: Characterisation of peripartum cardiomyopathy by cardiac magnetic resonance imaging. Eur Radiol 2009, 19:1324–132.

[51] Ricke-Hoch M, Bultmann I, Stapel B, Condorelli G, Rinas U, Sliwa K, Scherr M, Hilfiker-Kleiner D: Opposing roles of Akt and STAT3 in the protection of the maternal heart from peripartum stress. Cardiovasc Res 2014, 101:587-96.

[52] Hilfiker-Kleiner D, Haghikia A, Nonhoff J, Bauersachs J: Peripartum cardiomyopathy: current management and future perspectives. Eur Heart J 2015, 36:1090-7.

[53] Methawasin M, Hutchinson KR, Lee EJ, Smith JE, 3rd, Saripalli C, Hidalgo CG, Ottenheijm CA, Granzier H: Experimentally increasing titin compliance in a novel mouse model attenuates the Frank-Starling mechanism but has a beneficial effect on diastole. Circ 2014, 129:1924-36.

[54] Agarkova I, Auerbach D, Ehler E, Perriard J-C: A Novel Marker for Vertebrate Embryonic Heart, the EH-myomesin Isoform. J Biol Chem 2000, 275:10256–64.

[55] Lahmers S, Wu Y, Call DR, Labeit S, Granzier H: Developmental control of titin isoform expression and passive stiffness in fetal and neonatal myocardium. Circ Res 2004, 94:505-13.

[56] Freiburg A, Trombitas K, Hell W, Cazorla O, Fougerousse F, Centner T, Kolmerer B, Witt C, Beckmann JS, Gregorio CC, Granzier H, Labeit S: Series of Exon-Skipping Events in the Elastic Spring Region of Titin as the Structural Basis for Myofibrillar Elastic Diversity. Circ Res 2000, 86:1114-21.

[57] Agarkova I, Schoenauer R, Ehler E, Carlsson L, Carlsson E, Thornell L-E, Perriard J-C: The molecular composition of the sarcomeric M-band correlates with muscle fiber type. Eur J Cell Biol 2004, 83:193-204.

[58] Thum T, Galuppo P, Wolf C, Fiedler J, Kneitz S, van Laake LW, Doevendans PA, Mummery CL, Borlak J, Haverich A, Gross C, Engelhardt S, Ertl G, Bauersachs J: MicroRNAs in the human heart: a clue to fetal gene reprogramming in heart failure. Circ 2007, 116:258-67.

[59] Schoenauer R, Bertoncini P, Machaidze G, Aebi U, Perriard JC, Hegner M, Agarkova I: Myomesin is a molecular spring with adaptable elasticity. J Mol Biol 2005, 349:367-79.

[60] Obermann WMJ, Gautel M, Weber K, Fürst DO: Molecular structure of the sarcomeric M band: mapping of titin and myosin binding domains in myomesin and the identification of a potential regulatory phosphorylation site in myomesin. The EMBO Journal 1997, 16:211–20.

[61] Fukuzawa A, Lange S, Holt M, Vihola A, Carmignac V, Ferreiro A, Udd B, Gautel M: Interactions with titin and myomesin target obscurin and obscurin-like 1 to the M-band: implications for hereditary myopathies. Journal of Cell Science 2008, 121:1841-51.

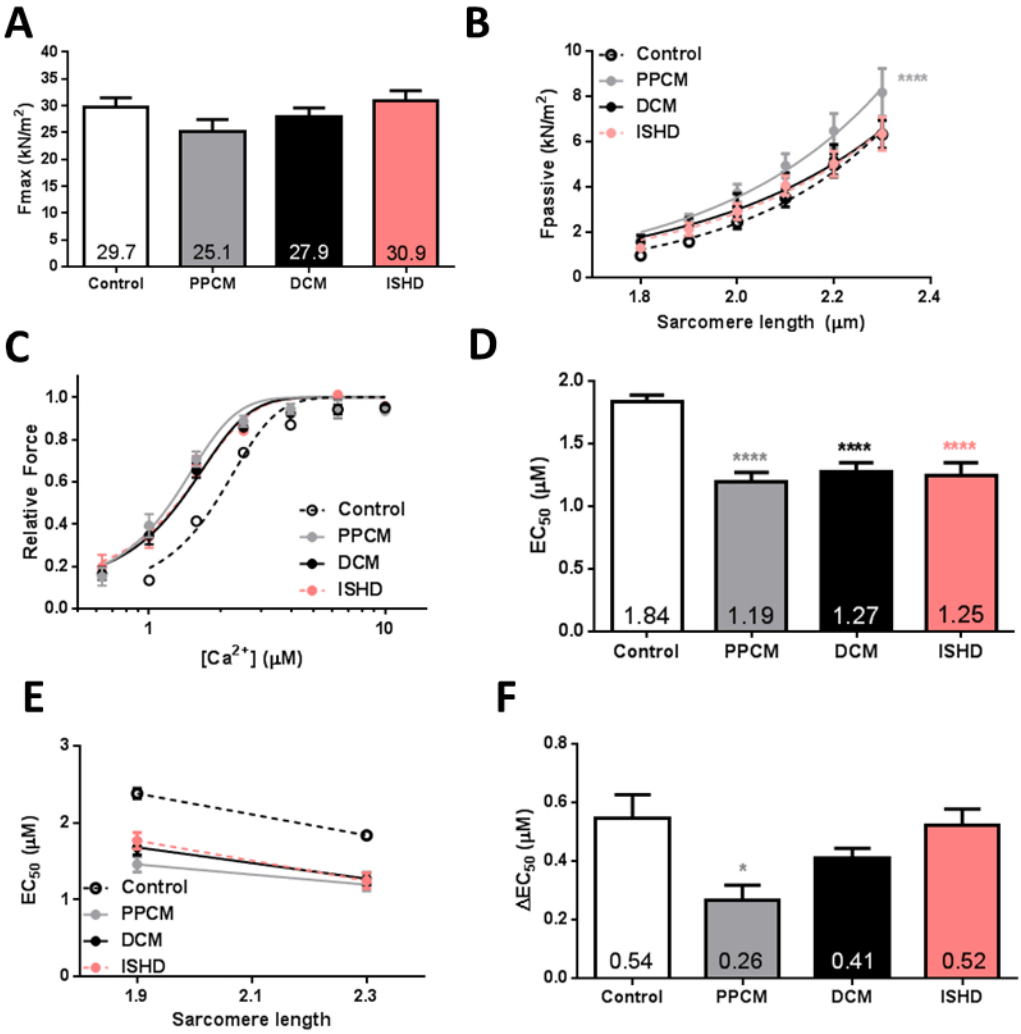
A
Fmax (kN/m²)
40
35
30
25
20
15
10
5
0
29.7
25.1
27.9
30.9
Control
PPCM
DCM
ISHD
B
Fpassive (kN/m²)
10
8
6
4
2
0
Control
PPCM
DCM
ISHD
****
1.8
2.0
2.2
2.4
Sarcomere length (µm)
C
Relative Force
1.0
0.8
0.6
0.4
0.2
0.0
Control
PPCM
DCM
ISHD
1
10
[Ca2+] (µM)
D
EC50 (µM)
2.0
1.5
1.0
0.5
0.0
****
****
****
1.84
1.19
1.27
1.25
Control
PPCM
DCM
ISHD
E
EC50 (µM)
3
2
1
0
Control
PPCM
DCM
ISHD
1.9
2.1
2.3
Sarcomere length
F
ΔEC50 (µM)
0.8
0.6
0.4
0.2
0.0
*
0.54
0.26
0.41
0.52
Control
PPCM
DCM
ISHD

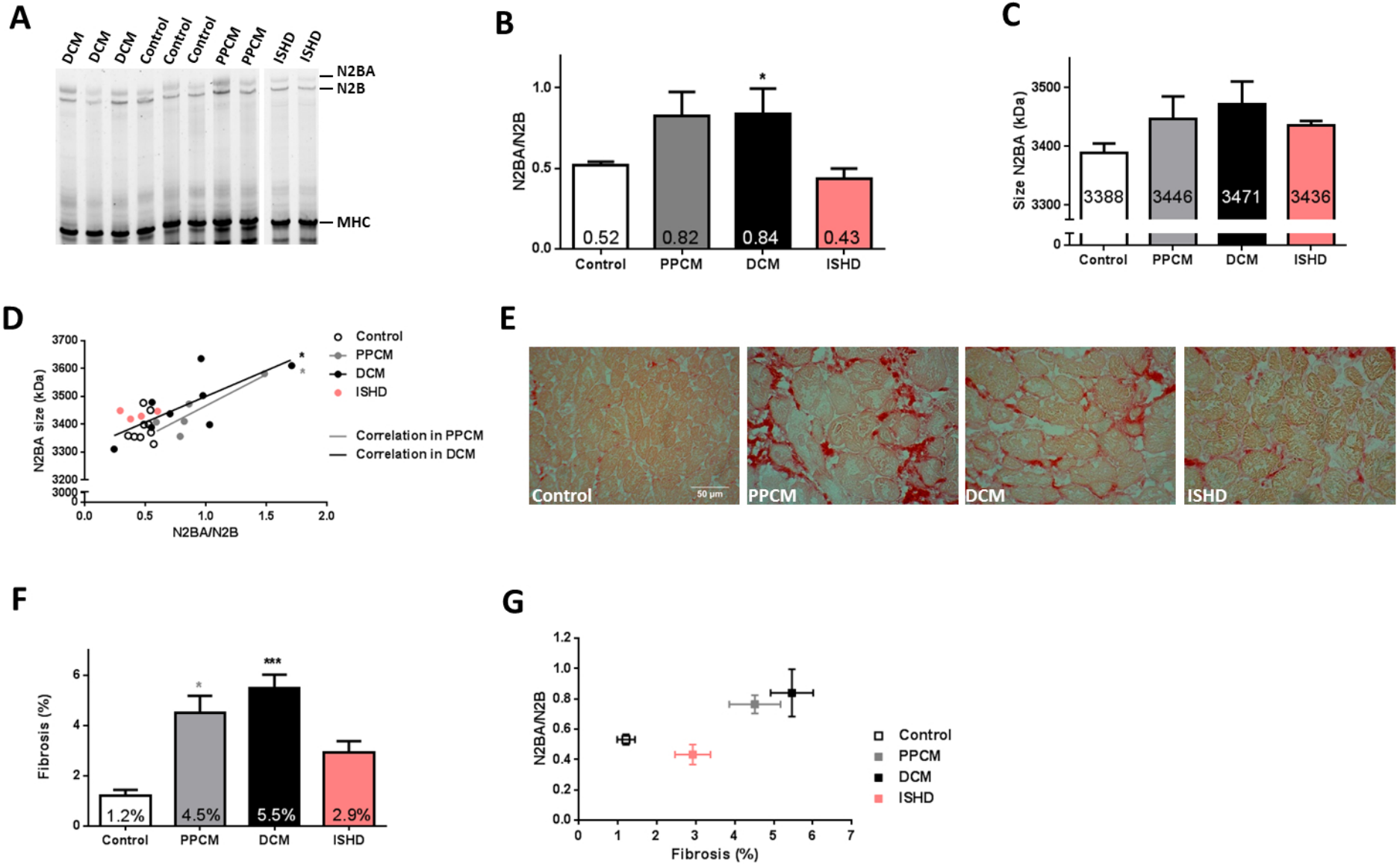
A
DCM
DCM
DCM
Control
Control
Control
PPCM
PPCM
ISHD
ISHD
N2BA
N2B
MHC
B
N2BA/N2B
1.0
0.5
0.0
0.52
0.82
0.84
0.43
*
Control
PPCM
DCM
ISHD
C
Size N2BA (kDa)
3500
3400
3300
0
3388
3446
3471
3436
Control
PPCM
DCM
ISHD
D
N2BA size (kDa)
3700
3600
3500
3400
3300
3200
3000
0
0.0
0.5
1.0
1.5
2.0
N2BA/N2B
Control
PPCM
DCM
ISHD
Correlation in PPCM
Correlation in DCM
E
Control
50 µm
PPCM
DCM
ISHD
F
Fibrosis (%)
6
4
2
0
1.2%
4.5%
5.5%
2.9%
*
***
Control
PPCM
DCM
ISHD
G
N2BA/N2B
1.2
1.0
0.8
0.6
0.4
0.2
0.0
0
1
2
3
4
5
6
7
Fibrosis (%)
Control
PPCM
DCM
ISHD

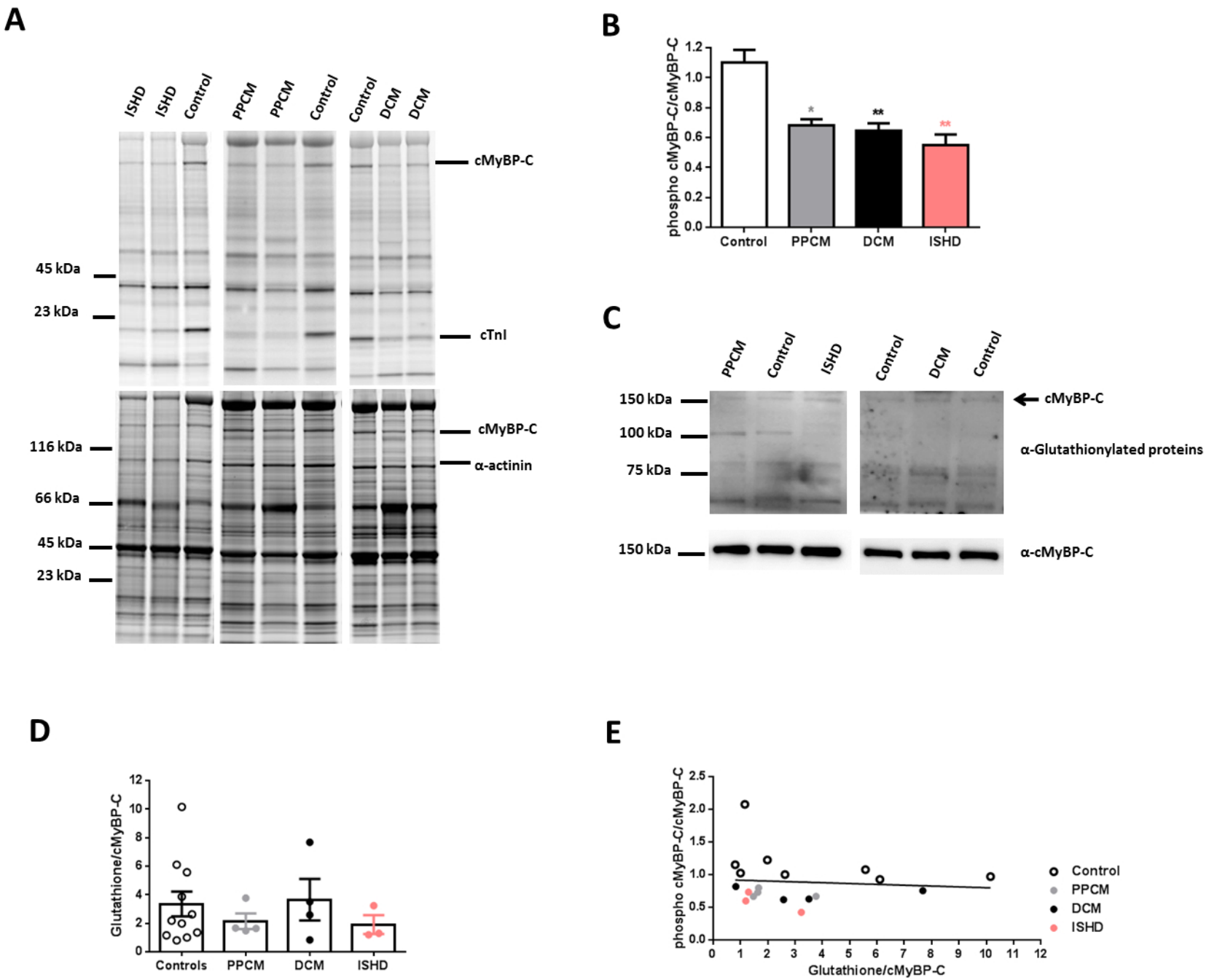
A
ISHD
ISHD
Control
PPCM
PPCM
Control
Control
DCM
DCM
cMyBP-C
cTnI
45 kDa
23 kDa
cMyBP-C
α-actinin
116 kDa
66 kDa
45 kDa
23 kDa
B
phospho cMyBP-C/cMyBP-C
1.2
1.0
0.8
0.6
0.4
0.2
0.0
*
**
**
Control
PPCM
DCM
ISHD
C
PPCM
Control
ISHD
Control
DCM
Control
150 kDa
100 kDa
75 kDa
cMyBP-C
α-Glutathionylated proteins
150 kDa
α-cMyBP-C
D
Glutathione/cMyBP-C
12
10
8
6
4
2
0
Controls
PPCM
DCM
ISHD
E
phospho cMyBP-C/cMyBP-C
2.5
2.0
1.5
1.0
0.5
0.0
0
1
2
3
4
5
6
7
8
9
10
11
12
Glutathione/cMyBP-C
Control
PPCM
DCM
ISHD

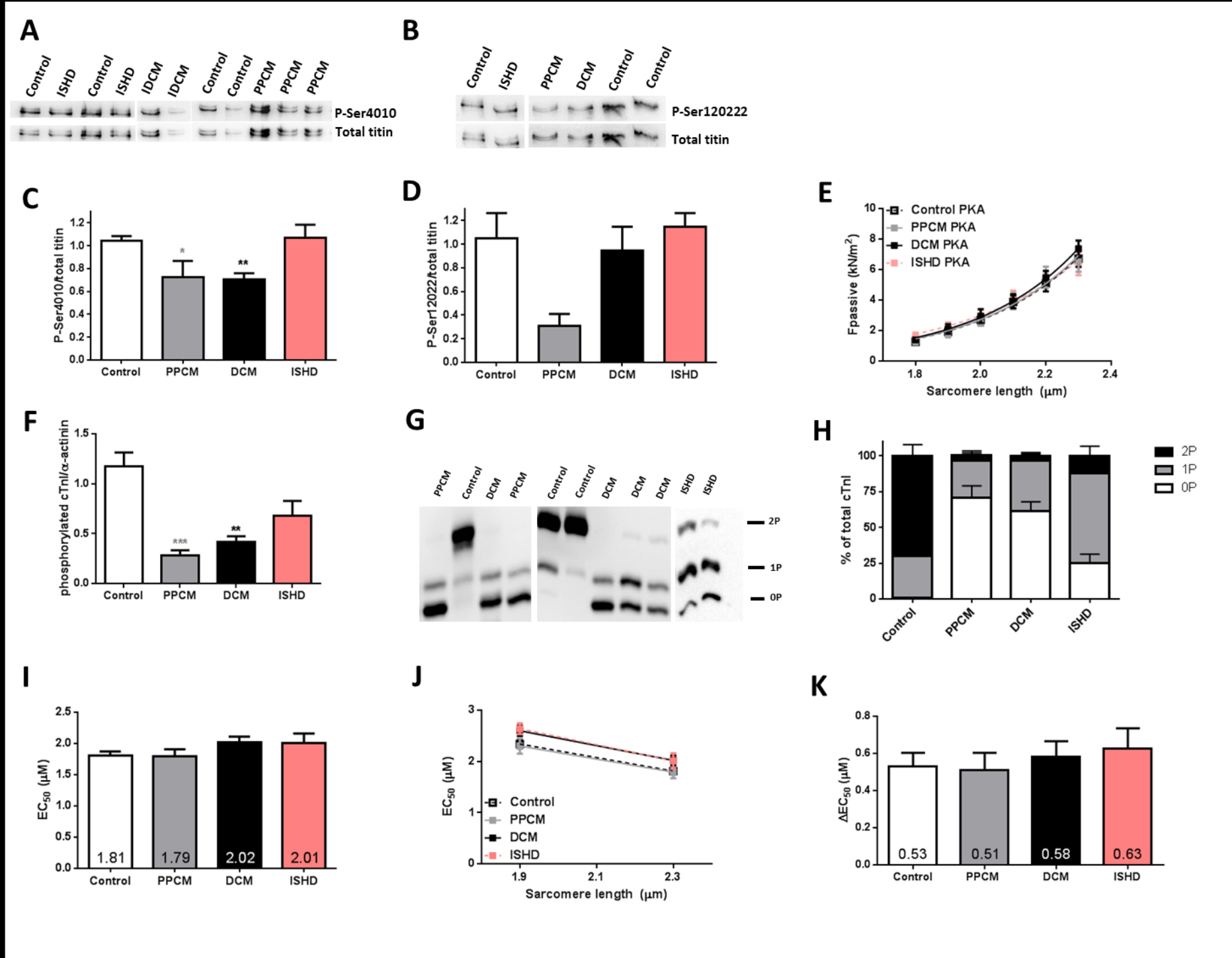
A
Control
ISHD
Control
ISHD
IDCM
IDCM
Control
Control
PPCM
PPCM
PPCM
P-Ser4010
Total titin
B
Control
ISHD
PPCM
DCM
Control
Control
P-Ser120222
Total titin
C
P-Ser4010/total titin
Control
PPCM
DCM
ISHD
D
P-Ser12022/total titin
Control
PPCM
DCM
ISHD
E
Control PKA
PPCM PKA
DCM PKA
ISHD PKA
Fpassive (kN/m²)
Sarcomere length (μm)
F
phosphorylated cTnI/α-actinin
Control
PPCM
DCM
ISHD
G
PPCM
Control
DCM
PPCM
Control
Control
DCM
DCM
DCM
ISHD
ISHD
2P
1P
0P
H
% of total cTnI
2P
1P
0P
Control
PPCM
DCM
ISHD
I
EC50 (μM)
1.81
1.79
2.02
2.01
Control
PPCM
DCM
ISHD
J
EC50 (μM)
Control
PPCM
DCM
ISHD
Sarcomere length (μm)
K
ΔEC50 (μM)
0.53
0.51
0.58
0.63
Control
PPCM
DCM
ISHD

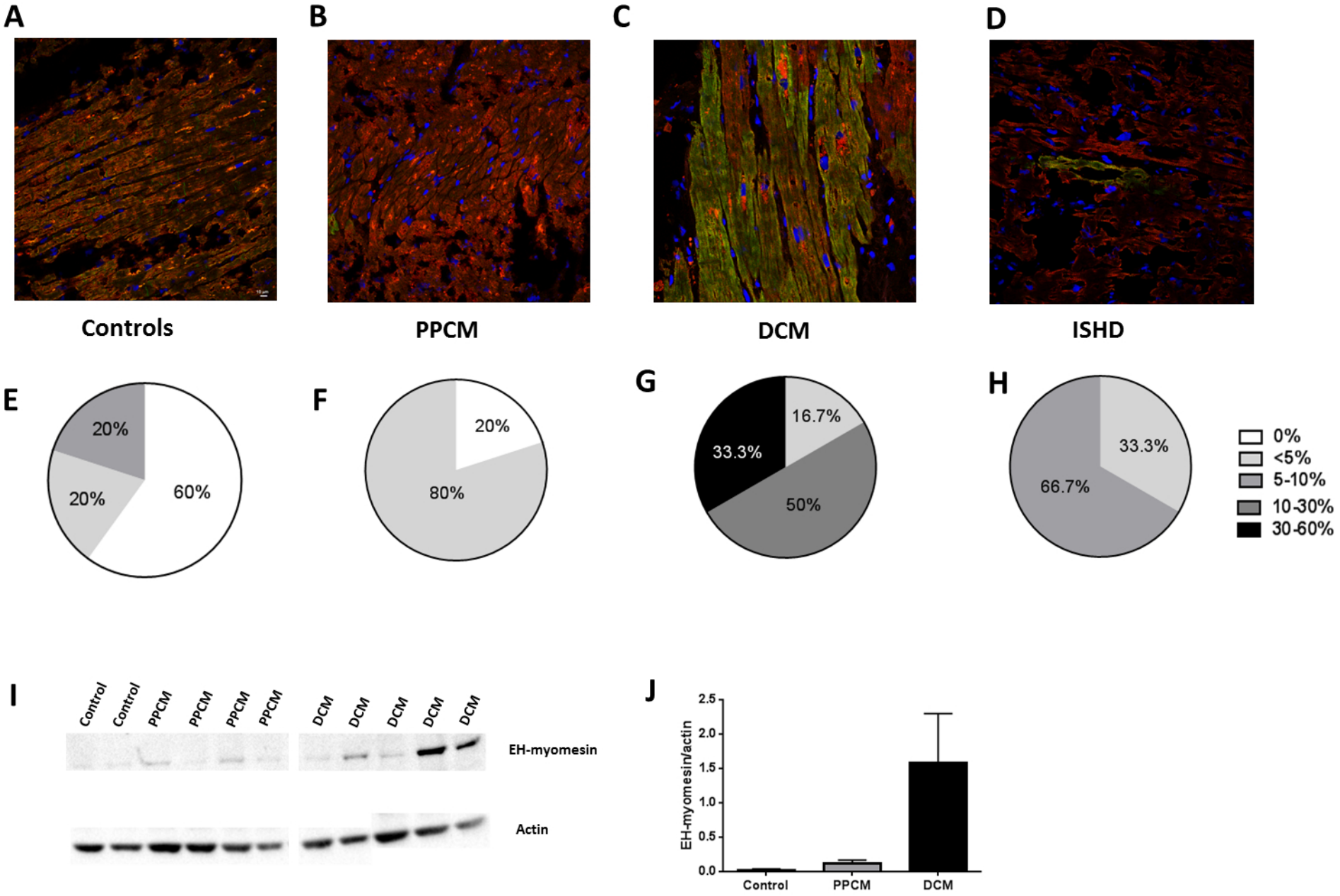
A
B
C
D
Controls
PPCM
DCM
ISHD
E
20%
20%
60%
F
20%
80%
G
16.7%
33.3%
50%
H
33.3%
66.7%
0%
<5%
5-10%
10-30%
30-60%
I
Control
Control
PPCM
PPCM
PPCM
PPCM
DCM
DCM
DCM
DCM
DCM
EH-myomesin
Actin
J
EH-myomesin/actin
2.5
2.0
1.5
1.0
0.5
0.0
Control
PPCM
DCM

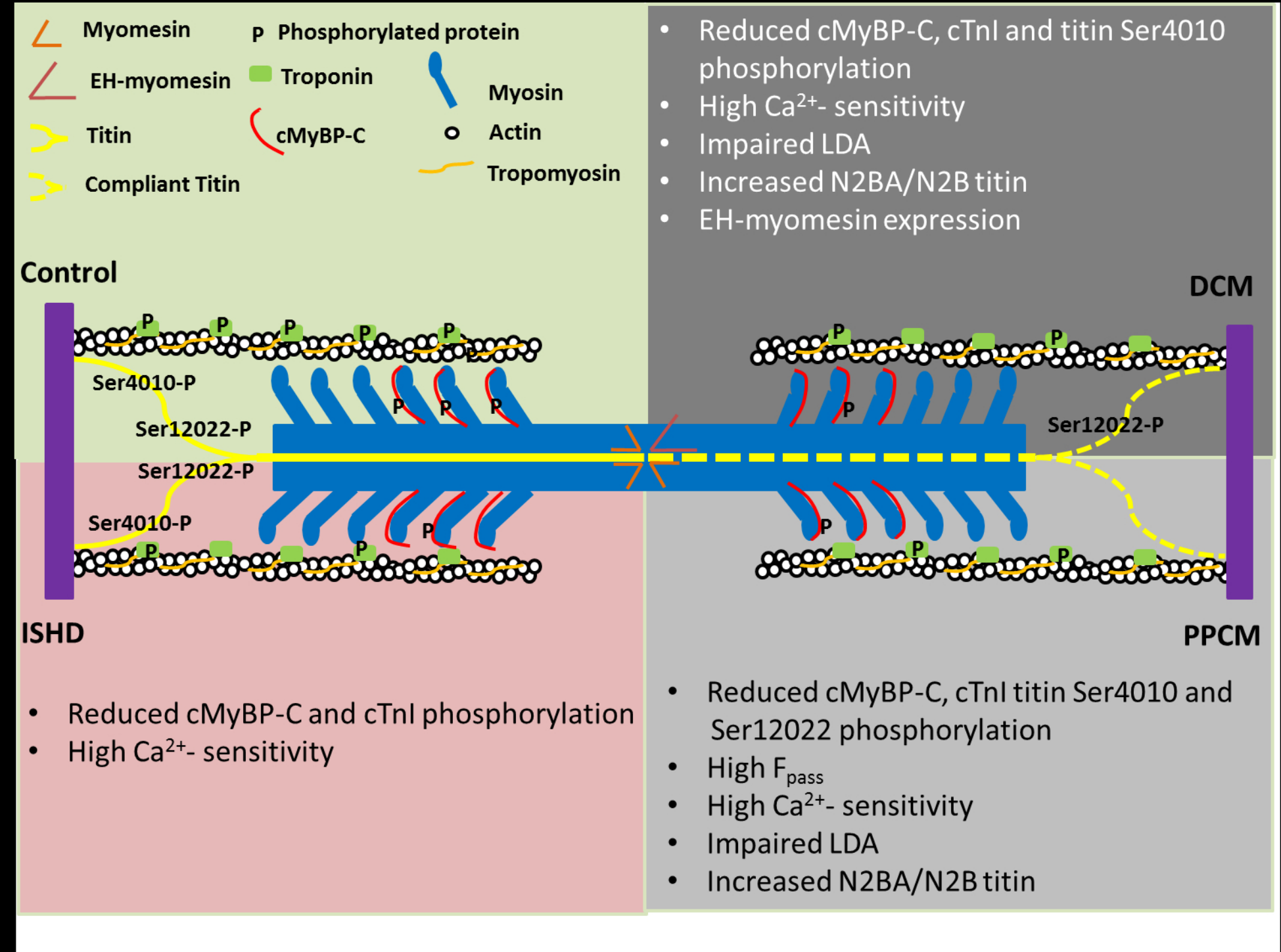


- Reduced cMyBP-C, cTnI and titin Ser4010 phosphorylation
- High $Ca^{2+}$- sensitivity
- Impaired LDA
- Increased N2BA/N2B titin
- EH-myomesin expression

- Reduced cMyBP-C and cTnI phosphorylation
- High $Ca^{2+}$- sensitivity

- Reduced cMyBP-C, cTnI titin Ser4010 and Ser12022 phosphorylation
- High $F_{pass}$
- High $Ca^{2+}$- sensitivity
- Impaired LDA
- Increased N2BA/N2B titin

**Supplemental Figure legends**

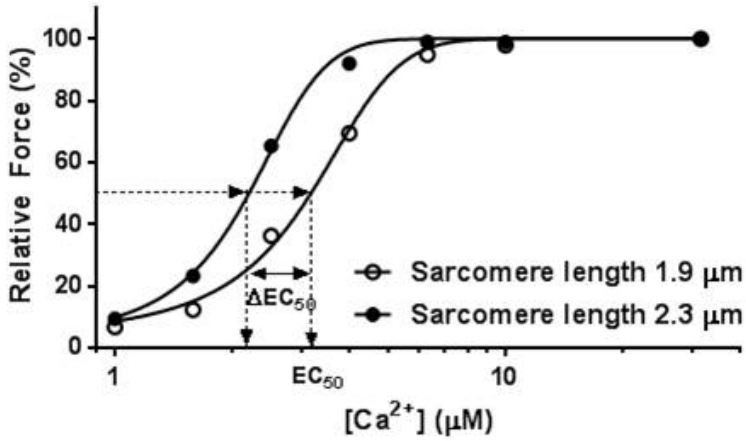


**Supplemental Figure 1. Assessment of $Ca^{2+}$-sensitivity, $EC_{50}$ and length-dependent activation**

Representatve relative force-[$Ca^{2+}$] curves are shown of a permeabilized cardiomyocyte measured at sarcomere length 1.9 µm and 2.3 µm. Force of each cell was normalized to its $F_{max}$ at both lengths. $Ca^{2+}$-sensitivity was expressed as the [$Ca^{2+}$] needed to achieve 50% of $F_{max}$ ($EC_{50}$) and length-dependent activation was measured as the shift in $EC_{50}$ ($\Delta EC_{50}$) at a sarcomere length of 1.9 µm and 2.3 µm.

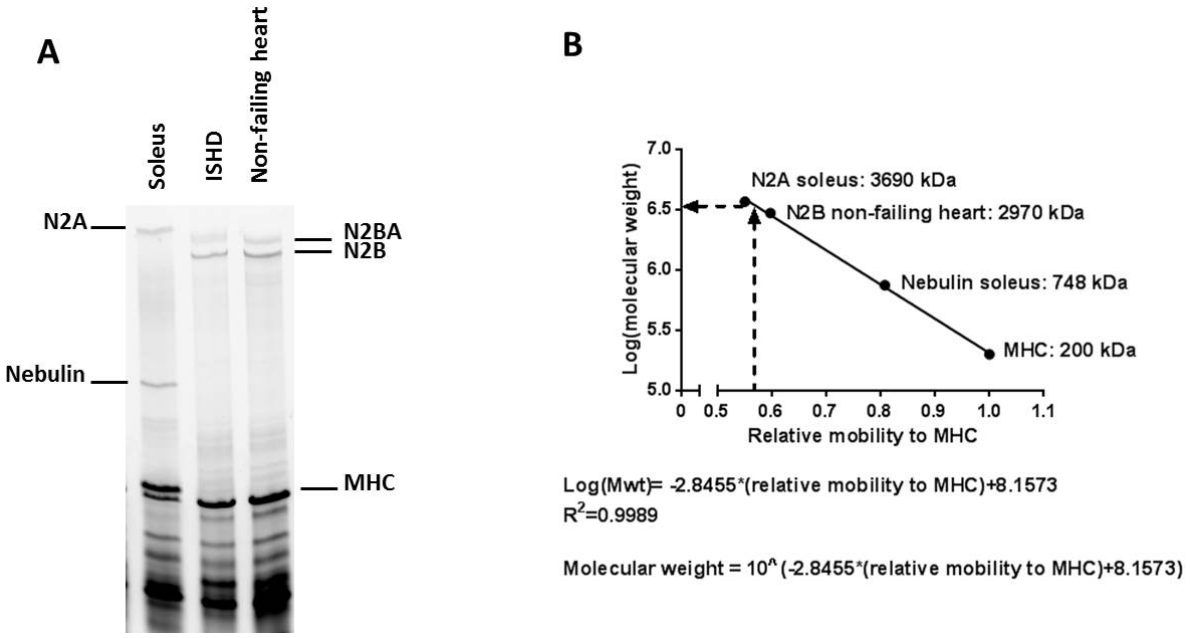


**Supplemental Figure 2. Determination of titin size.**

**A:** Titin isoforms were separated on a 1% agarose gel with electrophoresis. **B:** A calibration curve was constructed based on mobility of proteins of known molecular weight (N2A soleus 3690 kDa; N2B non-failing heart 2970 kDa; nebulin soleus muscle 748 kDa and myosin heavy chain (MHC) 200 kDa) relative to MHC. In order to avoid gel-to-gel variation or variation in mobility within a gel, only the adjacent lanes were used for the construction of the calibration curve. This calibration curve was used to calculate the molecular weight of the N2BA titin band of the sample of interest based on relative mobility to MHC.

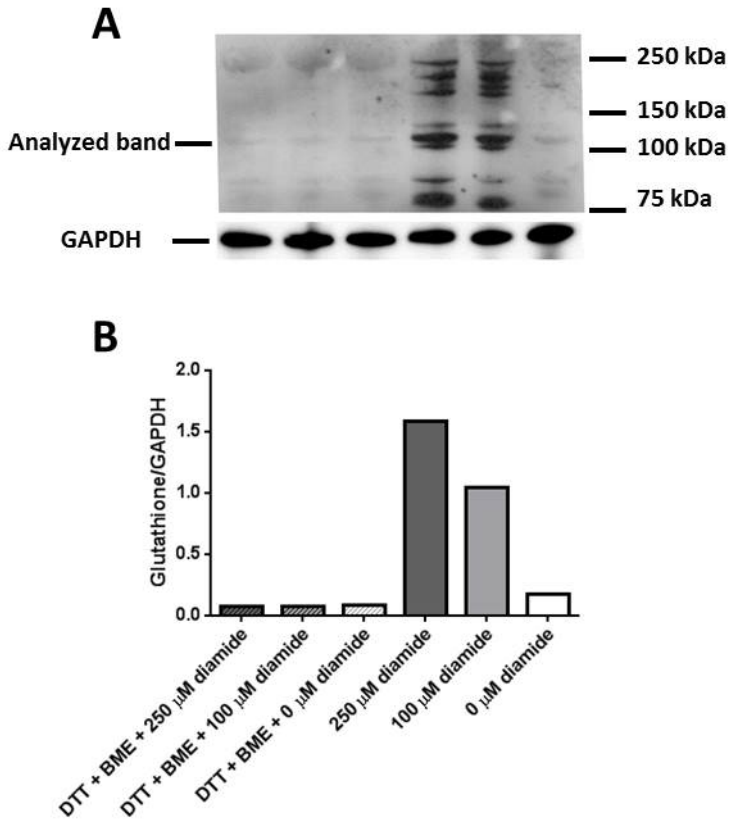


**Supplemental Figure 3. Positive and negative controls for glutathionylation western blots**

**A:** Positive and negative controls were produced by treating isolated adult rat cardiomyocytes with reducing or oxidizing compounds. Negative controls were obtained by treating homogenates with the reducing compounds DTT and BME. Positive controls showed increased glutathione signal after incubation with diamide, a inducer of glutathionylation, in a dose dependent manner. **B**: Quantified glutathionylation of positive and negative controls. The band used for analysis is indicated in **A**.